Changes in Miniature Endplate Potential Frequency during Repetitive Nerve Stimulation in the Presence of Ca^{2+}, Ba^{2+}, and Sr^{2+} at the Frog Neuromuscular Junction

J. E. ZENGEL and K. L. MAGLEBY

From the Department of Physiology and Biophysics, University of Miami School of Medicine, Miami, Florida 33101. J. E. Zengel's present address is the Departments of Neuroscience and Neurosurgery, University of Florida College of Medicine, Gainesville, Florida 32610.

ABSTRACT Miniature endplate potentials (MEPPs) were recorded from frog sartorious neuromuscular junctions under conditions of reduced quantal contents to study the effect of repetitive nerve stimulation on asynchronous (tonic) quantal transmitter release. MEPP frequency increased during repetitive stimulation and then decayed back to the control level after the conditioning trains. The decay of the increased MEPP frequency after 100- to 200-impulse conditioning trains can be described by four components that decayed exponentially with time constants of about 50 ms, 500 ms, 7 s, and 80 s. These time constants are similar to those for the decay of stimulation-induced changes in synchronous (phasic) transmitter release, as measured by endplate potential (EPP) amplitudes, corresponding, respectively, to the first and second components of facilitation, augmentation, and potentiation. The addition of small amounts of Ca^{2+} or Ba^{2+} to the Ca^{2+}-containing bathing solution, or the replacement of Ca^{2+} with Sr^{2+}, led to a greater increase in the stimulation-induced increases in MEPP frequency. The Sr-induced increase in MEPP frequency was associated with an increase in the second component of facilitation of MEPP frequency; the Ba-induced increase with an increase in augmentation. These effects of Sr^{2+} and Ba^{2+} on stimulation-induced changes in MEPP frequency are similar to the effects of these ions on stimulation-induced changes in EPP amplitude. These ionic similarities and the similar kinetics of decay suggest that stimulation-induced changes in MEPP frequency and EPP amplitude have some similar underlying mechanisms. Calculations are presented which show that a fourth-power residual calcium model for stimulation-induced changes in transmitter release cannot readily account for the observation that stimulation-induced changes in MEPP frequency and EPP amplitude have similar time-courses.

INTRODUCTION

Quantal transmitter release at the neuromuscular junction can be divided into two types: synchronous (phasic) release, which produces endplate potentials

J. GEN. PHYSIOL. © The Rockefeller University Press · 0022-1295/81/05/0503/27 $1.00 503
Volume 77 May 1981 503-529

(EPPs), and asynchronous (tonic) release, which produces miniature endplate potentials (MEPPs) (del Castillo and Katz, 1954 *a*; Boyd and Martin, 1956; Miledi and Thies, 1971; Silinisky et al., 1977). Under conditions of reduced quantal content, repetitive stimulation of the motor nerve leads to cumulative increases in both types of release; EPP amplitudes increase during repetitive stimulation, and testing impulses applied after the conditioning trains show that the altered state of the nerve terminal that gives rise to this increased transmitter release returns slowly to the preconditioning level (Feng, 1941; Liley, 1956; Gage and Hubbard, 1966; Braun, et al., 1966). Similarly, the frequency of MEPPs increases during repetitive stimulation and returns to the prestimulation levels after the conditioning trains (del Castillo and Katz, 1954 *a*; Liley, 1956; Hubbard, 1963; Hurlbut et al., 1971; Miledi and Thies, 1971; Erulkar and Rahamimoff, 1978). In this paper we examine the kinetic properties and ionic dependence of stimulation-induced changes in MEPP frequency and compare them to stimulation-induced changes in EPP amplitude to investigate whether the two types of transmitter release underlying these phenomena have mechanisms in common. A preliminary report of this study has appeared (Zengel and Magleby, 1978).

METHODS

Standard microelectrode techniques were used to record intracellular endplate potentials (EPPs) and miniature endplate potentials (MEPPs) from endplate regions of frog (*Rana pipiens*) sartorius nerve-muscle preparations (Magleby and Zengel, 1976 *a*). Most experiments were performed with 6- to 8-MΩ electrodes on muscles from medium sized frogs (~3 inches from nose to rump). MEPP amplitudes tended to be small (0.1–0.5 mV), because the muscle fibers were large (see Katz and Thesleff [1957]), but the noise level in the recording system was low because of the low-resistance electrodes, and it was usually possible to hold such cells for 1–5 h with resting potentials more negative than −70 to −80 mV.

The standard bathing solution had the composition (mM); NaCl, 115; KCl, 2; $CaCl_2$, 1.8; Na_2HPO_4, 2.16; NaH_2PO_4, 0.85; glucose, 5; choline, 0.03. This solution was modified by reducing Ca^{2+} to 0.3–0.6 mM and adding 5 mM Mg^{2+} to greatly decrease quantal content (low-Ca Ringer's solution). Osmolarity was maintained by changing NaCl. To examine the effects of Ba^{2+} and Sr^{2+}, the low-Ca Ringer's solution was modified by adding 0.1–0.2 mM Ba^{2+} or 0.2–0.4 mM Sr^{2+}, or by replacing the Ca^{2+} with 0.8–1.2 mM Sr^{2+} (Sr Ringer's solution). The pH of all solutions was adjusted to 7.2–7.4 before use. Experiments were carried out at 20°C.

In the basic experiment described in this paper we investigated the effects of the solutions on the time-course of changes in MEPP frequency that occur during and after repetitive stimulation. Data were collected and analyzed in terms of trials, each trial consisting of a period before the conditioning train to determine the control MEPP frequency, a conditioning train, and a period of time after the train to follow the decay of MEPP frequency back to control levels. Trials with short conditioning trains (10–11 impulses) usually lasted 30 s. Trials with long conditioning trains (100–200 impulses) usually lasted 5–8 min.

In preliminary experiments, MEPPs were recorded with an FM tape recorder, played into a penwriter at reduced tape speed, and analyzed by hand. The results of these experiments were consistent with those presented in this paper, but it was not

practical using this technique to obtain and analyze enough data to define reliably the time-course of changes in MEPP frequency. To solve this problem, we and Dr. Frank Morris developed a computer program that delivered the desired stimulation pattern to the nerve and recorded the amplitude of all the resulting EPPs and the amplitude and time of occurrence (1-ms resolution) of all MEPPs. MEPPs were detected by their amplitudes and rates of rise and decay. The program also detected MEPPs that fell on the decaying phase (tails) of EPPs or other MEPPs; it measured the amplitude of these MEPPs by assuming an exponential decay of the preceding EPP or MEPP. The time constant of decay used in the program was determined for each cell from the decay of EPPs in that cell. The base line toward which the voltage decayed was updated as the program ran to correct for possible drifts in the resting potential and recording system.

This program was extensively tested by comparing computer-measured results with those obtained by measuring the same data by hand. The two methods gave virtually

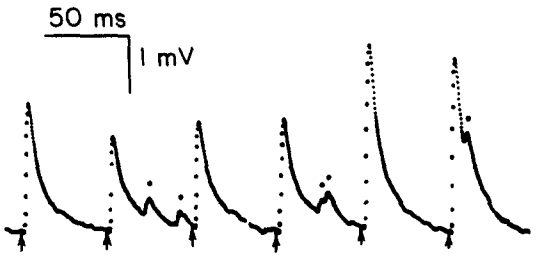

FIGURE 1. Detection of MEPPs during a conditioning train. Computer-sampled and -displayed data from an intracellular record obtained from the endplate region of a frog sartorius nerve-muscle preparation. The response to six stimuli near the end of a 40-impulse train is shown. The arrows indicate the time of the nerve impulses delivered at a rate of 20/s. The responses immediately after the stimuli are EPPs. The responses with dots above them (computer placed) are computer-detected MEPPs. To facilitate photography, the data were obtained from a tape-recorded experiment. The sample rate in this illustration (1 point/250 μs) was two to four times faster than that normally used during direct computer-sampled experiments. 0.5 mM Ca^{2+}.

identical results. During an experiment, the computer continuously displayed the digitized data and placed a dot over each detected MEPP, so the accuracy of detection could be continuously monitored.

Fig. 1 presents examples of computer-sampled data during a conditioning train of 40 impulses delivered at 20 impulses/s. The arrows indicate the time of nerve stimulation; the responses immediately after the arrows are EPPs. The dots above the smaller potentials indicate computer-detected MEPPs. Notice that the program detects all MEPPs, including those occurring during the falling phase of EPPs or previous MEPPs. The signal, as was the case for Fig. 1, was usually filtered with a low-pass active filter (18 dB/octave) at 500 Hz before analysis to reduce unwanted noise. This slowed the rise of the MEPPs and EPPs somewhat but had little effect on their peak amplitudes. The threshold level for MEPP detection was set to exclude the ciass of very small MEPPs described by Kriebel and Gross (1974).

After the experiments, the data from all trials to be averaged were superimposed in

a master file by arranging all MEPPs for all the trials in order of their time of occurrence in relation to the start of each trial. Each MEPP was stored as a time of occurrence together with its amplitude. Plots of MEPP frequency against time were then made from this master file. MEPP rate during the conditioning train was corrected to compensate for the fact that MEPPs could not be detected during the time required to stimulate the nerve and sample for EPPs (usually ~6–10 ms, depending on the length of the nerve and the resulting conduction time).

Preliminary analysis of the data was carried out by the moving bin technique, which has been described in detail by Rahamimoff and Yaari (1973). Basically, the frequency of MEPPs was calculated for a block of time (bin size), and the block was then advanced (moved) in time with steps smaller than the bin size. The frequency of MEPPs was plotted at the center of the time bin for each successive position. To increase the resolution of this technique, we further analyzed the data using a modified moving bin technique in which the bin size was changed according to the rate and rate of change of MEPP frequency. Large bin sizes (200 ms to several seconds) were used when the MEPP frequency was low and only slowly changing with time, such as before a conditioning train or several seconds after the train. Smaller bin sizes (10–200 ms) were used when the frequency of MEPPs was high and/or rapidly changing in time, such as during and immediately after the conditioning trains. For the data analysis for most of the figures in this paper we used a changing bin size with steps in time of about one-half to one times the current bin size. This increased the time resolution where necessary and simplified the figures by decreasing the number of points to be plotted. We also analyzed much of the data with standard moving bin and nonmoving bin techniques, with similar results.

Data are presented as mean ± SD.

RESULTS

MEPP Frequency Increases during and after Repetitive Stimulation

The effect of repetitive stimulation on the frequency of MEPPs is shown in Fig. 2. The nerve was conditioned with 1,000 impulses applied at a rate of 20 impulses/s. Intracellular records obtained at various times during (*A–C*) and after(*D–F*) the conditioning train are presented. Responses whose rising phases fell between 2 and 6 ms after each stimulus (indicated by the rapid vertical deflections) were considered to be EPPs; the other responses, indicated by the dots, were considered to be MEPPs. In addition to the stimulation-induced increase in EPP amplitudes, the MEPP frequency increased from <1/s at the start of the train (Fig. 2 *A*) to ~15/s after 41 s of stimulation (Fig. 2 *C*). After the conditioning train, the MEPP frequency returned slowly toward the control frequency (Fig. 2 *D–F*). The marked fluctuation in successive EPP amplitudes during the train was due to the quantal nature of transmitter release (del Castillo and Katz, 1954 *a*), which is very evident at the low quantal contents used in these experiments. A stimulation-induced increase in evoked and spontaneous transmitter release was consistently seen in the more than 30 experiments performed for this study. The amplitudes of MEPPs did not change during or after the conditioning stimulation in these experiments, in agreement with previous studies (del Castillo and Katz, 1954 *b*; Magleby

and Zengel, 1976 *a*), indicating that postsynaptic sensitivity remained constant under the low quantal content conditions.

Decay of MEPP Frequency after Repetitive Stimulation Described by Four Exponential Components

Because of the small number of MEPPs that occur during and after any single conditioning train, it was not possible to obtain accurate estimates of the time-course of changes in MEPP frequency from a single conditioning trial such as that shown in Fig. 2. This difficulty was overcome by combining data from

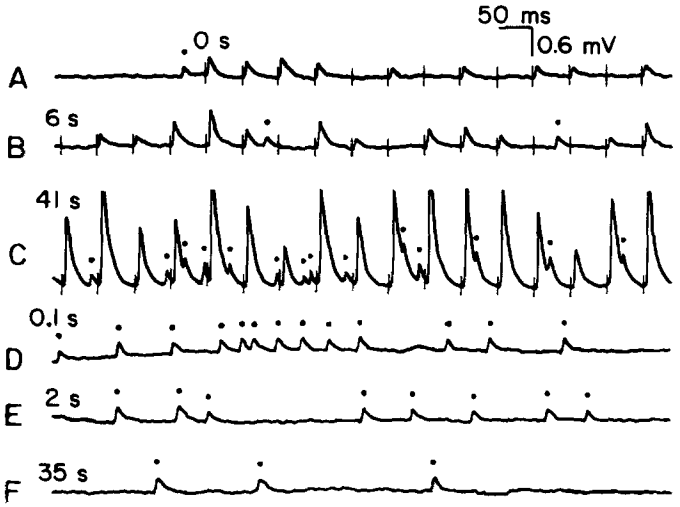

FIGURE 2. Effect of repetitive nerve stimulation on EPP amplitude and MEPP frequency. Tracings of intracellular recordings. The nerve was conditioned with 1,000 impulses at a rate of 20 impulses/s. The records were obtained at the indicated times during (*A–C*) and after (*D–F*) the conditioning train. The sharp vertical deflections (shock artifacts) indicate the times of the stimuli. Responses immediately after the stimuli are EPPs. The dots indicate MEPPs. The flat-topped EPPs in *C* are due to the pen writer reaching its limit of travel. 0.4 mM Ca^{2+}.

many identical conditioning-testing trials. An example is shown in Fig. 3, which presents data from 123 trials in which a total of 47,295 MEPPs were recorded. Each trial consisted of a 30-s rest period before the conditioning train to obtain estimates of the control MEPP rate, a 200-impulse conditioning train delivered at 20 impulses/s, and a 5-min period to measure the decay of MEPP frequency after the conditioning train. Average MEPP frequency increased more than 10 times during the conditioning train and then decayed back to the control level with several apparent time constants (Fig. 3 *A*).

To analyze the decay of MEPP frequency we began by expressing MEPP frequency as $V_M(t)$, the fractional increase in MEPP frequency over the

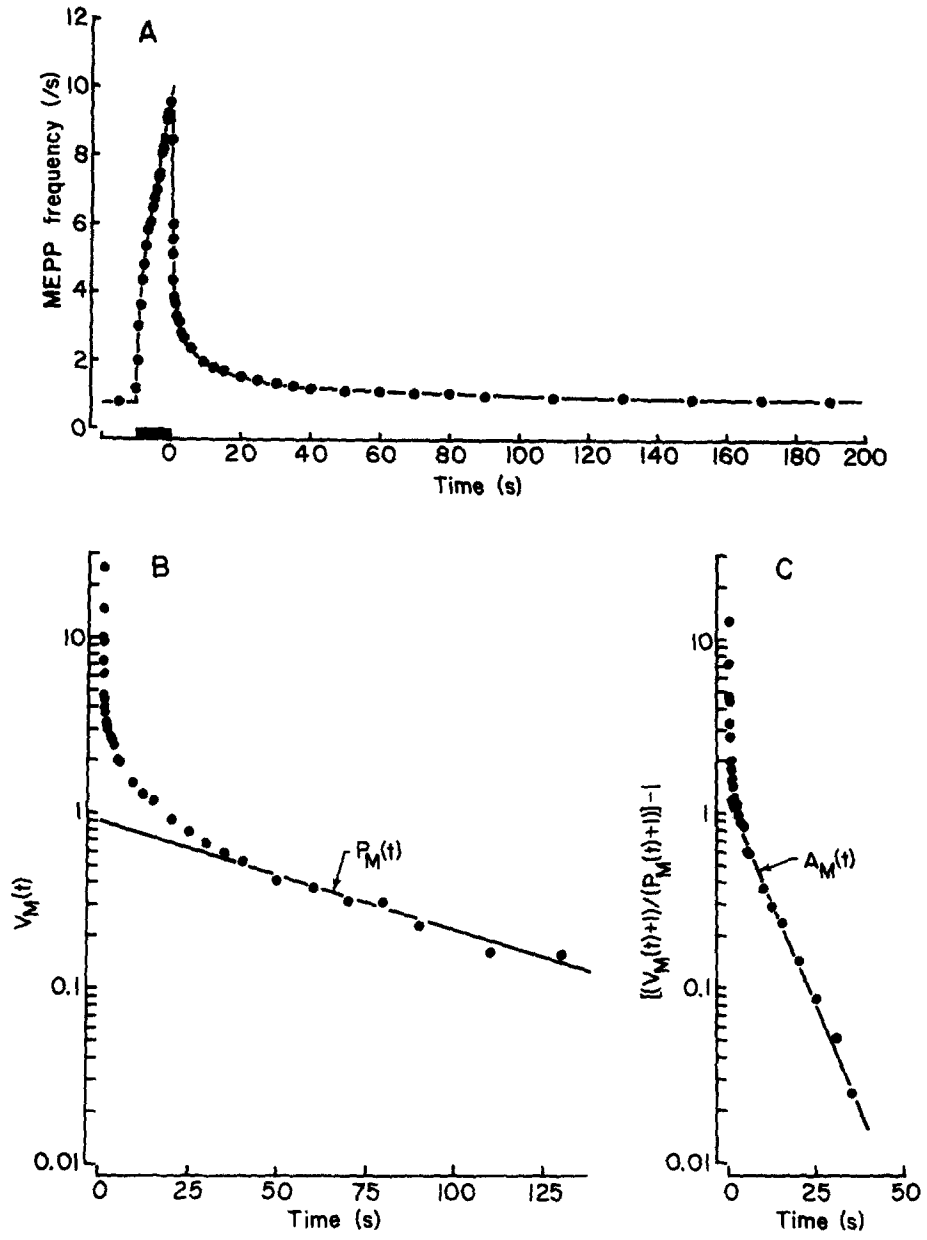

FIGURE 3.

control, such that

$$V_M(t) = \frac{v_M(t)}{v_{M_0}} - 1, \tag{1}$$

where $v_M(t)$ is the MEPP frequency at time t and v_{M_0} is the control MEPP frequency. $V_M(t)$ was then plotted semilogarithmically against time as shown

in Fig. 3 *B*. The line in this figure represents the exponential decay of the slowest component of MEPP frequency, which had a time constant (time required to fall to $1/e$ of its initial value) of 69 s. The magnitude of this component, 0.9, was obtained by extrapolating the line to 0 time, the time at the end of the conditioning train.

Superimposed on this slowest decaying component were faster decaying components, as indicated by the deviation of the data points from the line at times <30 s. Because the faster decaying components fell on one or more

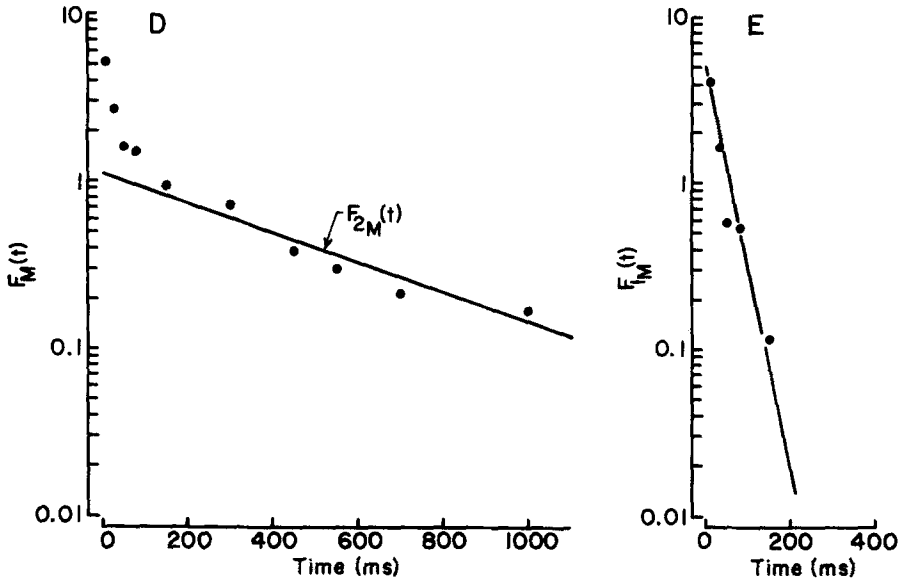

FIGURE 3. Effect of 200-impulse conditioning trains (20 impulses/s) on MEPP frequency. Data averaged from 12 cells from six preparations (123 trials, 47,295 MEPPs). (*A*) Rise and decay of MEPP frequency during and after the conditioning stimulation, which is indicated by the horizontal bar. (*B*) Decay of the fractional increase in MEPP frequency, $V_M(t)$, after the conditioning train shown in *A*. The line indicates the decay of potentiation, $P_M(t)$, the slowest component. The decay of MEPP frequency was well described by this line to 250 s after the train (data only plotted to 130 s), at which time the increased frequency was too small to measure. (*C*) Decay of the increase in MEPP frequency after the data in *B* had been corrected for the contribution of $P_M(t)$ with Eq. 2. The line plots the decay of augmentation, $A_M(t)$, the next slowest component. (*D* and *E*) Decay of the faster components, the second component of facilitation, $F_{2_M}(t)$, and the first component of facilitation, $F_{1_M}(t)$, obtained after the data in C had been corrected for $A_M(t)$. In this and the following figures the bin sizes used in the data analysis were often different for the various parts of the figures; the bin sizes were typically smaller immediately after the train in those parts where higher time resolution was needed, such as *B* when compared with *A*. Decay lines have been drawn by eye. 0.4 mM Ca^{2+}. The quantal content in the absence of repetitive stimulation ranged from 0.1 to 1.2 in the cells averaged for this figure for an overall average of ~0.4.

slower decaying components, estimates of these faster decaying components could only be obtained in terms of a model that defined the way in which the different components combined to change MEPP frequency. We initially analyzed the data in three ways: by assuming additive, multiplicative, and power relationships among the different components (similar to Eqs. 6, 7, and 8 in Zengel and Magleby [1980]); in all cases, the decay of MEPP frequency was well described by four exponentially decaying components with time constants similar to those of the four components of stimulation-induced changes in EPP amplitude.

Because of this similarity and the observation that the model used to analyze the decays had little effect on the time constants of decay of the four components, we refer to components of MEPP frequency by the names of the similarily decaying components of EPP amplitude, and we have analyzed the decays of MEPP frequency presented in the figures and table in this paper in the manner used previously to account for and analyze stimulation-induced changes in EPP amplitudes (Zengel and Magleby, 1977 and 1980) so that direct comparisons between these two types of transmitter release could be made. (Support for the implied assumption in this analysis that analogous components of MEPP frequency and EPP amplitude have similar underlying mechanisms will be presented in the following sections.)

The data were analyzed with

$$V_M(t) = [F_{1_M}(t) + F_{2_M}(t) + 1]^3[A_M(t) + 1][P_M(t) + 1] - 1, \qquad (2)$$

where $V_M(t)$ is the fractional increase in MEPP frequency as defined by Eq. 1, $F_{1_M}(t)$ and $F_{2_M}(t)$ are the first and second components of facilitation of MEPP frequency, $A_M(t)$ is augmentation of MEPP frequency, and $P_M(t)$ is the potentiation component (see Eq. 7 in Zengel and Magleby [1980]).

$P_M(t)$, the slowest decaying component, was estimated as shown in Fig. 3 *B* from the decay of the fractional increase in MEPP frequency after the facilitation and augmentation components had decayed to insignificant levels.

Fig. 3 *C* presents a semilogarithmic plot of the faster decaying components of MEPP frequency after correction for $P_M(t)$. The points plotted in this figure were calculated from $\{[V_M(t) + 1]/[P_M(t) + 1]\} - 1$ using values of $V_M(t)$ obtained from the observed MEPP frequency with Eq. 1 and values of $P_M(t)$ determined from the line in Fig. 3 *B*. The line in Fig. 3 *C* indicates the decay of $A_M(t)$, the second slowest component of MEPP frequency, which had a time constant of 9.1 s.

The two slowest decaying components of MEPP frequency, indicated by the lines in Fig. 3 *B* and *C* (potentiation and augmentation, respectively), are similar to those described by Erulkar and Rahamimoff (1978) and apparent in the data of Liley (1956).

The deviation of MEPP frequency at short times from the line describing the decay of $A_M(t)$ in Fig. 3 *C* indicates the presence of still faster decaying components of MEPP frequency. Rearranging Eq. 2 to solve for facilitation gave $F_{1_M}(t) + F_{2_M}(t) = \{[V_M(t) + 1]/\{[A_M(t) + 1][P_M(t) + 1]\}\}^{1/3} - 1$. Values of the sum of the two components of facilitation, $F_M(t)$, were calculated

from this equation and plotted semilogarithmically against time in Fig. 3 *D*, using values of $V_M(t)$ obtained from the observed MEPP frequency with Eq. 1 and values of $P_M(t)$ and $A_M(t)$ determined from the lines in Fig. 3 *B* and *C*, respectively. The line in Fig. 3 *D* indicates the decay of the second component of facilitation of MEPP frequency, which had a time constant of 565 ms. Subtracting this line from the data points at short times and replotting them in Fig. 3 *E* gave the decay of the first component of facilitation of MEPP frequency, which had a time constant of 44 ms.

Four components of decay of MEPP frequency were seen in three other experiments of the type shown in Fig. 3. The two slower components were also present in other experiments in which there were not enough MEPPs to analyze for the faster components. Data from all of these experiments are summarized in Table I. For comparison, the time constants for the decay of the first component of facilitation, the second component of facilitation, augmentation, and potentiation of EPP amplitude are also presented. Notice

TABLE I

TIME CONSTANTS OF DECAY OF THE FOUR COMPONENTS OF TONIC AND PHASIC QUANTAL TRANSMITTER RELEASE AFTER 100- to 200-IMPULSE CONDITIONING TRAINS

Component	MEPP frequency		EPP amplitude*	
Facilitation				
First component, *ms*	47±9‡	(4)	60±12	(7)
Second component, *ms*	472±108	(4)	508±87	(7)
Augmentation, *s*	6.9±1.6	(11)	7.3±1.3	(52)
Potentiation, *s*	82±25	(19)	65±18	(52)

Number of estimates is indicated in parentheses.

* From Magleby and Zengel (1976 *a*), Zengel and Magleby (1980), and unpublished observations.

‡ Mean ± SD.

that the four time constants that describe the decay of MEPP frequency are similar to the four time constants describing the decay of EPP amplitude. This similarity of time constants suggests that corresponding components of decay of MEPP frequency and EPP amplitude may have similar mechanisms. If this is the case, corresponding components should also have similar ionic sensitivities. This possibility is examined in the following sections.

Sr^{2+} Increases the Magnitude and Time Constant of Decay of the Second Component of Facilitation of MEPP Frequency

The addition of small amounts of Sr^{2+} to the bathing solution or the replacement of Ca^{2+} with Sr^{2+} increases the magnitude and time constant of decay of the second component of facilitation of EPP amplitude but has little effect on potentiation, augmentation, or the first component of facilitation (Zengel and Magleby, 1977 and 1980). Fig. 4 shows that Sr^{2+} has a similar effect on the second component of facilitation of MEPP frequency. Intracellular re-

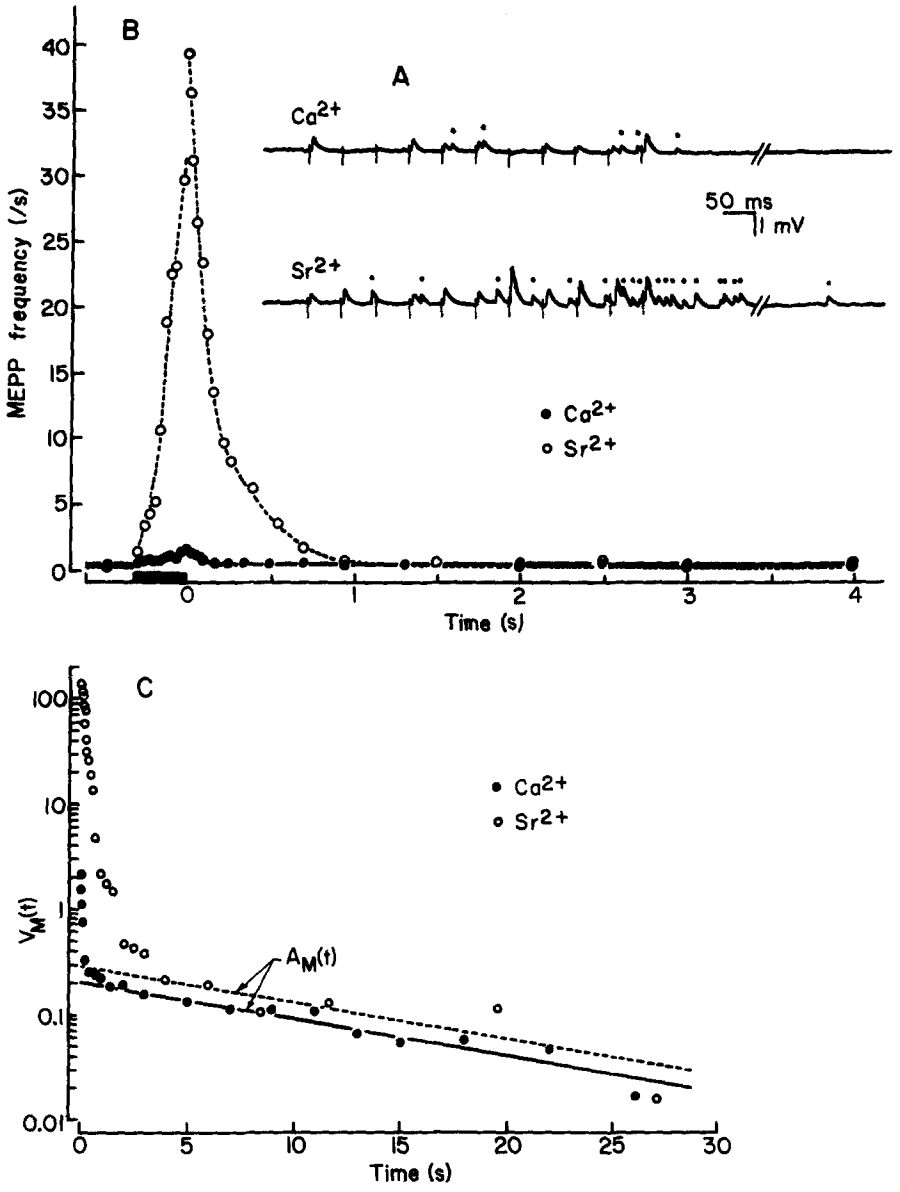

FIGURE 4.

cordings obtained during and after 11-impulse conditioning trains in low-Ca (0.55 mM) Ringer's solution (low-Ca Ringer) and after replacement of the Ca^{2+} with 1.2 mM Sr^{2+} are shown in Fig. 4 *A*. There was a much greater increase in MEPP frequency during and immediately after the conditioning train recorded in Sr^{2+}. This enhancement of MEPP frequency by Sr^{2+} was no longer detectable ~1 s after the train (after the break in the base line). This observation suggests that Sr^{2+} increased facilitation of MEPP frequency,

which would be expected to decay in <1–2 s but had little effect on the slower decaying augmentation and potentiation of MEPP frequency.

That this is the case is shown in Fig. 4 *B–E*. In this experiment, the nerve was conditioned with 11 impulses at 33 impulses/s. Fig. 4 *B* shows plots of MEPP frequency against time during and after conditioning trains in low-Ca (0.5 mM) Ringer (filled circles) and 0.9 mM Sr Ringer's solution (Sr Ringer) (open circles). Although there was little difference in the control MEPP frequency for the two solutions (0.47/s in low-Ca Ringer and 0.31/s in Sr

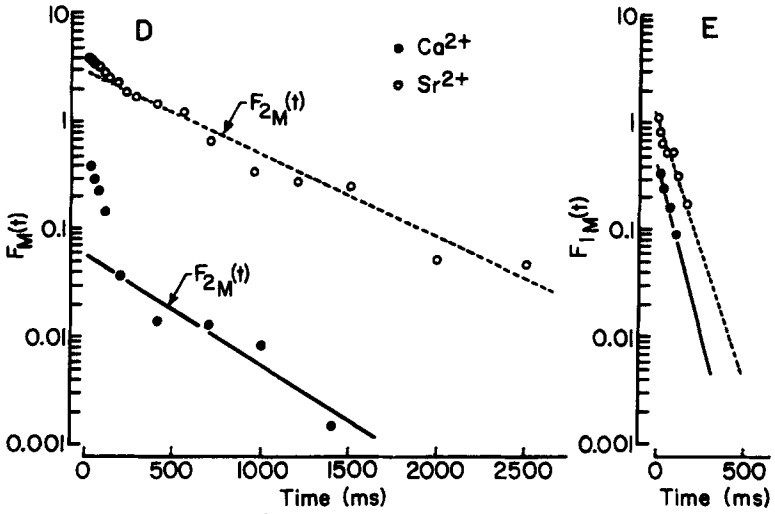

FIGURE 4. Effect of Sr^{2+} on the stimulation-induced increase in MEPP frequency during and after short conditioning trains. (*A*) Tracings of intracellular records obtained during and after conditioning trains of 11 impulses delivered at 20 impulses/s in low-Ca (0.55 mM) Ringer and after the replacement of Ca^{2+} with 1.1 mM Sr^{2+}. The breaks in the records exclude 500 ms. (*B*) Rise and decay of MEPP frequency during and after conditioning trains of 11 impulses delivered at 33 impulses/s in low-Ca (0.5 mM) Ringer (filled circles) and in 0.9 mM Sr Ringer (open circles). The Ca data were averaged from four cells from two preparations (961 trials, 15,547 MEPPs), and the Sr data from two cells from one preparation (53 trials, 1,204 MEPPs). (*C*) Decay of the increase in MEPP frequency, $V_M(t)$, after the train in *B*. The decays of augmentation, $A_M(t)$, in low-Ca Ringer (continuous line) and Sr Ringer (dashed line) are shown. (*D* and *E*) Decay of the second component of facilitation, $F_{2_M}(t)$, and the first component of facilitation, $F_{1_M}(t)$, obtained from the data in *C* after correction for $A_M(t)$.

Ringer), MEPP frequency increased to >30/s by the end of the conditioning train in Sr Ringer, compared with an increase to only 2/s in low-Ca Ringer.

Fig. 4 *C–E* shows plots of the decay of augmentation and the two components of facilitation of MEPP frequency after the conditioning trains shown in Fig. 4 *B*. Notice in Fig. 4 *D* that Sr^{2+} increased the magnitude of the second component of facilitation immediately after the conditioning train 50 times, from 0.056 to 2.8, while increasing its time constant of decay about 1.4 times, from 420 to 574 ms. Compared with these dramatic effects on the second

component of facilitation, Sr^{2+} had relatively little effect on augmentation (Fig. 4 *C*) or on the first component of facilitation (Fig. 4 *E*). (The magnitude of potentiation after these 11-impulse trains was small and not included in the analysis.)

When the data were analyzed assuming an additive relationship (Zengel and Magleby, 1980) between the components of MEPP frequency instead of the relationship described by Eq. 2, a similar selective effect of Sr^{2+} was observed. Sr^{2+} increased the magnitude of the second component of facilitation over 450 times while having less of an effect (only 10% as great, 45 times increase) on the magnitude of the first component of facilitation and little effect (<1% as great, 1.5 times increase) on the magnitude of augmentation. The selective effect of Sr^{2+} on increasing the second component of facilitation of MEPP frequency was consistently observed, was reversible, and is similar to the effect of Sr^{2+} on stimulation-induced changes in EPP amplitude (cf. Fig. 4, this paper, and Fig. 7, Zengel and Magleby [1980]).

If the second component of facilitation of MEPP frequency has kinetics similar to those of the second component of facilitation of EPP amplitude, as suggested by the results presented in Fig. 4, then the Sr-induced increase in the second component of facilitation of MEPP frequency should occur mainly during the first 1–2 s of repetitive stimulation when the magnitude of this component is increasing toward a steady-state level. (See Mallart and Martin [1967] and Zengel and Magleby [1980] for a discussion of the kinetics of facilitation.) That this is the case is shown in Fig. 5, where it can be seen that the Sr-induced increase in MEPP frequency occurs mainly during the first 2 s of repetitive stimulation, similar to the Sr-induced increase in EPP amplitude (cf. Fig. 5, this paper, and Figs. 9 *A* and 10, Zengel and Magleby [1980]).

Analysis of the decay of MEPP frequency after long conditioning trains such as those used for Fig. 5 showed that, whereas Sr^{2+} increased the second component of facilitation of MEPP frequency, it had little effect on augmentation or potentiation of MEPP frequency.

Ba^{2+} Increases the Magnitude of Augmentation of MEPP Frequency

The addition of small amounts of Ba^{2+} to the bathing solution increases the magnitude of augmentation of EPP amplitude but has little effect on the time-course of augmentation or the magnitude or time-course of potentiation (Zengel and Magleby, 1980). If augmentation of MEPP frequency has an underlying mechanism similar to augmentation of EPP amplitude, then Ba^{2+} should also increase the magnitude of augmentation of MEPP frequency.

That this is the case is shown in Fig. 6. In this experiment, the nerve was stimulated with 100-impulse (20/s) conditioning trains in low-Ca (0.4 mM) Ringer and after the addition of 0.1 mM Ba^{2+} to the low-Ca Ringer. Fig. 6 *A* presents plots of the MEPP frequency during and after the conditioning trains. The MEPP frequency increased to 50/s by the end of the conditioning train recorded in the presence of Ba^{2+} (open circles), compared with an increase to only 8/s in its absence (filled circles).

In contrast to Sr^{2+}, which produced a greater rate of increase in MEPP

frequency, mainly during the first 1–2 s of repetitive stimulation (Fig. 5), Ba^{2+} produced a greater rate of increase in MEPP frequency throughout the conditioning train (Fig. 6 *B*). After the train, the Ba-induced increase in MEPP frequency decayed in ~20 s (Fig. 6 *A*), whereas the Sr-induced increase in MEPP frequency decayed in ~1 s (Fig. 4 *B*). These effects of Ba^{2+} would be expected if Ba^{2+} increased the magnitude of augmentation of MEPP frequency, since increased augmentation can lead to a greater rate of increase

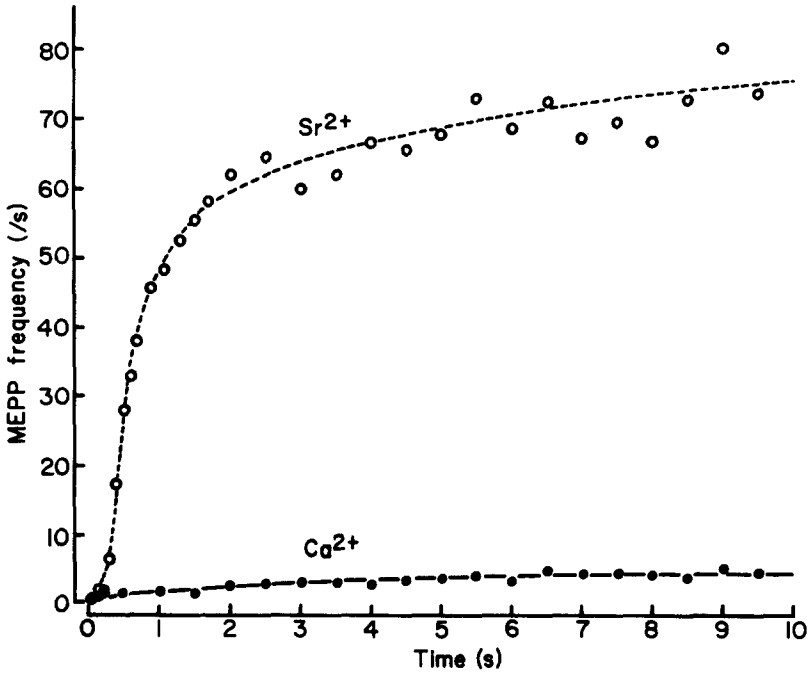

FIGURE 5. Effect of Sr^{2+} on the stimulation-induced increase in MEPP frequency during long conditioning trains. Plot of MEPP frequency against time during conditioning trains of 200 impulses delivered at 20 impulses/s in low-Ca (0.4 mM) Ringer (filled circles) and after the Ca^{2+} had been replaced with 0.8 mM Sr^{2+} (open circles). Average of six trials for the Ca data and seven trials for the Sr data, all obtained from the same cell.

in EPP amplitude during repetitive stimulation, which then mostly decays within 20 s after the train (Magleby and Zengel [1976 *b*], Figs. 1 and 3).

Fig. 6 *C* and *D* shows that Ba^{2+} did increase the magnitude of augmentation of MEPP frequency 17-fold, from ~0.9 to 15 (Fig. 6 *D*), but had little effect on potentiation (Fig. 6 *C*). In six experiments of the type shown in Fig. 6, Ba^{2+} increased the magnitude of augmentation of MEPP frequency 7.5 ± 5-fold (range of 4–16). The apparent Ba-induced increase in the time constant of decay of augmentation of MEPP frequency shown in Fig. 6 *D* was not consistently seen. In these same six experiments, the mean time constant of

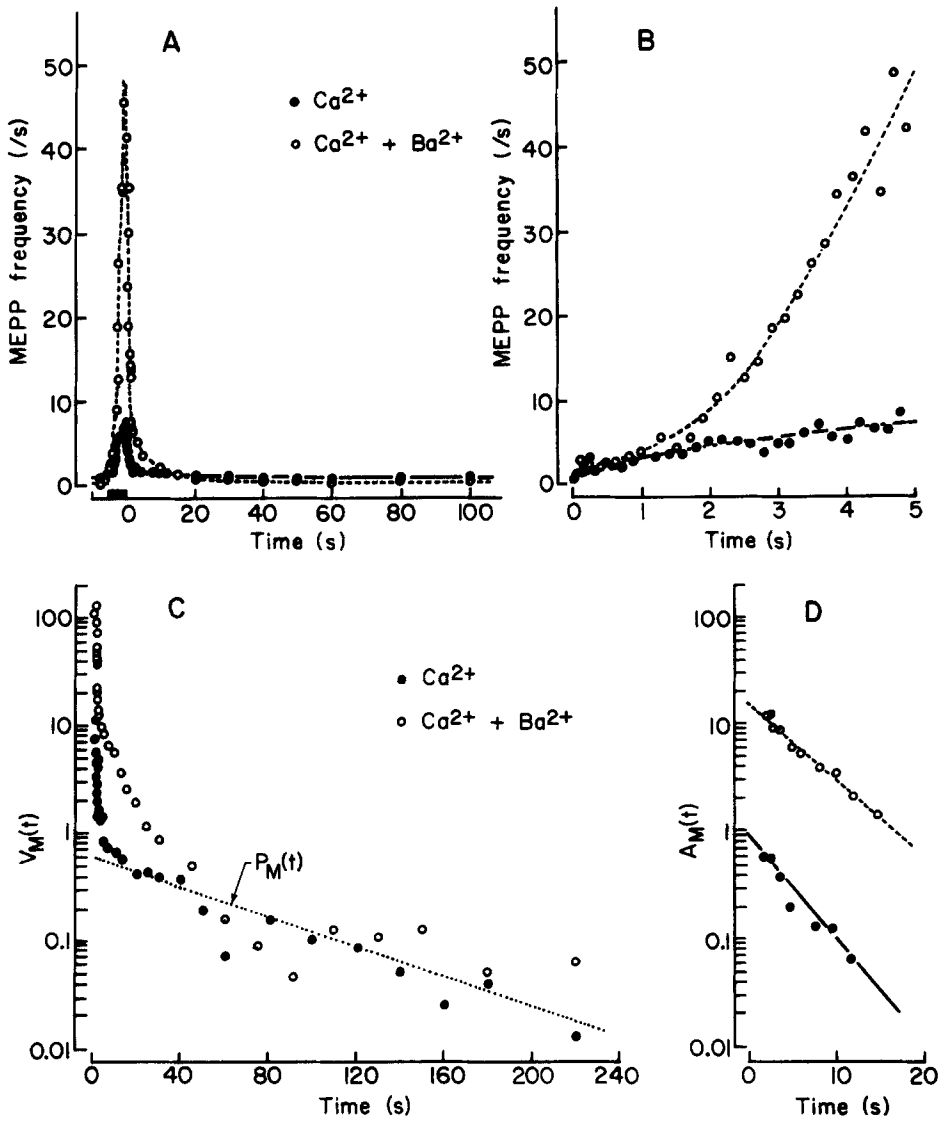

FIGURE 6. Effect of Ba^{2+} on the stimulation-induced increase in MEPP frequency. (*A*) Rise and decay of MEPP frequency during and after conditioning trains of 100 impulses delivered at 20 impulses/s in low-Ca (0.4 mM) Ringer (filled circles) and in 0.4 mM Ca^{2+} + 0.1 mM Ba^{2+} Ringer (open circles). Average of 15 trials (4,558 MEPPs) for the Ca data and 16 trials (3,957 MEPPs) for the Ca + Ba data, all recorded from the same cell. (*B*) Rise of MEPP frequency during the trains in *A* plotted on an expanded time scale. (*C*) Decay of the increased MEPP frequency, $V_M(t)$, after the trains shown in *A*. The dotted line plots the decay of potentiation, $P_M(t)$. (*D*) Decay of augmentation, $A_M(t)$, for the data in *C* after correction for $P_M(t)$.

decay was 6.6 ± 2.1 s in the absence of Ba^{2+} and 6.4 ± 1.5 s in its presence. Thus, the Ba-induced increase in MEPP frequency was similar to the Ba-induced increase in EPP amplitude; in both cases Ba^{2+} increased the magnitude of augmentation but had little effect on its time constant of decay or on potentiation (cf. Fig. 6, this paper, and Fig. 1, Zengel and Magleby [1980]). As was the case for EPP amplitude (see Fig. 2 in Zengel and Magleby [1980]), the Ba effect was slow in onset and slowly reversible.

We had difficulty gathering enough data to obtain accurate estimates of the effect of Ba^{2+} on facilitation. However, analysis of the available data indicated that whether Ba^{2+} had an effect on facilitation depended on the assumed relationship between the components of increased MEPP frequency. When the data in Fig. 6 were analyzed using Eq. 2, Ba^{2+} appeared to have little effect (<50% increase) on the magnitudes and time constants of decay of the two components of facilitation when compared with the 16 times increase in the magnitude of augmentation. When the data in Fig. 6 were analyzed assuming an additive relationship (see Eq. 6, Zengel and Magleby [1980]) between the components of increased MEPP frequency, Ba^{2+} still had little effect on potentiation, increased the magnitude of augmentation 20 times with little effect on its time constant of decay, and appeared to increase the magnitudes of both components of facilitation >20–50 times with comparatively little effect on their time constants of decay. Similarly, Ba^{2+} also increased the magnitude of the two components of facilitation of EPP amplitude when the data were analyzed assuming an additive model, but, in contrast to the pronounced effect of Ba^{2+} on facilitation of MEPP frequency with this model, the effect of Ba^{2+} on facilitation of EPP amplitude was small when compared with the Ba-induced increase in the magnitude of augmentation of EPP amplitude (Zengel and Magleby, 1980).

Each Nerve Impulse Adds a Step Increase in MEPP Frequency

The initial rapid decay of MEPP frequency after the last impulse in the conditioning trains shown in Figs. 3, 4, and 6 suggests that there should be some decay of MEPP frequency between impulses during repetitive stimulation. To investigate this possibility, we measured MEPP frequency in the intervals between successive nerve impulses during repetitive stimulation at 20 impulses/s. The results are shown in Fig. 7. To obtain enough MEPPs to detect possible changes in frequency, it was necessary to combine data from many identical conditioning trains. The data in this figure were averaged from 2,700 blocks of data, each 100 ms long. (100 blocks of data were obtained from each of 27 conditioning trains of 200 impulses each.) Fig. 7 plots averaged MEPP frequency against time for two successive intervals between nerve impulses. The vertical dashed lines indicate the time of the nerve impulses, which occurred every 50 ms. It can be seen that MEPP frequency, when averaged over all the conditioning trains, jumped from 2/s just before each impulse to 5/s just after each impulse. When data from the first and second halves of the conditioning trains were analyzed separately, average MEPP frequency jumped from 1/s just before to 3/s just after each impulse during

the first half of the trains and from 3/s just before to 7/s just after each impulse during the second half (not shown).

These data suggest that each nerve impulse in a conditioning train produces a step increase in MEPP frequency that then decays appreciably (due mainly to the decay of facilitation) during the interval before the next impulse. This fluctuating response is superimposed on an underlying response that slowly increases (due mainly to the increases in augmentation and potentiation) during the conditioning train. The plotted increase in MEPP frequency during the conditioning trains in Figs. 3, 4, and 6 thus represents the underlying response plus the average of the fluctuating response.

Note that the only real discontinuous changes in MEPP frequency during

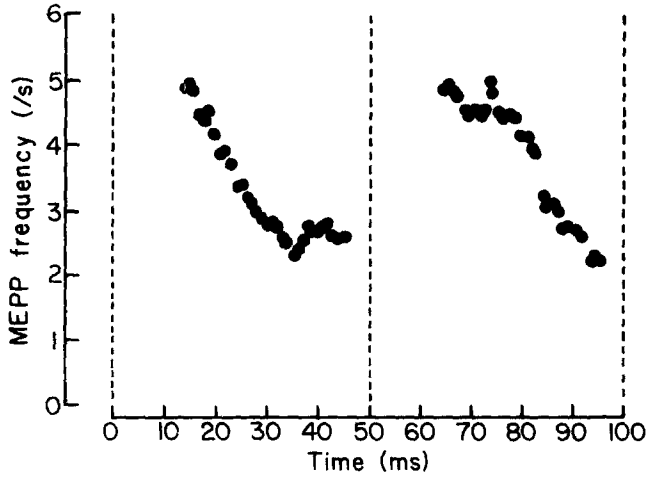

FIGURE 7. Changes in MEPP frequency between nerve impulses during repetitive stimulation. Consecutive 100-ms blocks of data were averaged from 27 conditioning trains of 200 impulses each (2,700 blocks of data, 770 MEPPs). The vertical dashed lines indicate the times of the nerve impulses in the 100-ms blocks of data. The plotted points, obtained using a bin size of 10 ms with a 1-ms step, show that each nerve impulse produces a rapid increase in average MEPP frequency, which then decays toward the initial level.

and after the conditioning trains were the incremental increases in MEPP frequency added by each nerve impulse. For example, MEPP frequency was higher immediately after (30-ms bin) rather than during the train shown in Fig. 4 *B* because of the incremental increase in MEPP frequency added by the last impulse in the train. Apparent discontinuities in MEPP frequency did appear, however, depending on the bin size used to average MEPPs during and after the conditioning trains. For example, large bin sizes (greater than the interval between nerve impulses during the train) led to an apparent sudden drop in MEPP frequency immediately after the conditioning trains. This occurred because the two components of facilitation of MEPP frequency, which were repeatedly added by each nerve impulse during the trains, decayed

rapidly after the trains and contributed little to measured MEPP frequency in the large bin after the trains. This is the case for Fig. 3 *A*, which shows an immediate drop in MEPP frequency after the train (200-ms bin).

If the bin size immediately after the train were made smaller than during the train, then the measured MEPP frequency immediately after the train was higher than that measured during the train. This occurred because the two components of facilitation added by the last impulse in the train did not have time to decay appreciably during the short measurement period immediately after the train. This is the case for the data analysis in Fig. 3 *B* when compared with Fig. 3 *A*, Fig. 4 *C* when compared with Fig. 4 *B*, and Fig. 6 *C* when compared with Fig. 6 *A* and *B*.

DISCUSSION

This study shows that stimulation-induced changes in MEPP frequency and EPP amplitude have similar decay rates and similar sensitivities to Ba^{2+} and Sr^{2+}. These findings suggest that stimulation-induced changes in these two types of transmitter release have some similar underlying mechanisms. This conclusion does not require that tonic and phasic quantal transmitter release have identical mechanisms; previous studies have suggested that the quanta used in the two types of release are not always identical (Dennis and Miledi, 1974; Large and Rang, 1978). It simply requires that both types of release are similar enough in underlying mechanisms that they respond in a similar manner to the stimulation-induced changes in the nerve terminal that increase release. Note that these conclusions apply only to *stimulation-induced changes* in MEPP frequency. It appears that a significant fraction of the resting MEPP frequency may be due to release mechanisms different from those that increase MEPP frequency during depolarization or stimulation of the nerve terminal (Barrett et al., 1978).

The demonstration that potentiation, augmentation, and the two components of facilitation are present after repetitive stimulation and that they retain their kinetic properties in the absence of testing nerve impulses shows that these processes are not due to changes in the size or shape of the presynaptic nerve action potential. This conclusion agrees with those drawn in previous studies using a variety of experimental techniques (Martin and Pilar, 1964; Braun and Schmidt, 1966; Zucker, 1974; Erulkar and Rahamimoff, 1978; Zucker and Lara-Estrell, 1979). Changes in the presynaptic nerve action potential may, however, modify some of these processes (Charlton and Bittner, 1978).

Previous studies (Rahamimoff and Yaari, 1973; McLachlan, 1977; Mellow et al., 1978; Silinsky, 1978) have established that Sr^{2+} and Ba^{2+} enhance stimulation-induced changes in MEPP frequency. This study shows that the Sr-induced increase in MEPP frequency during and after repetitive stimulation is associated mainly with an increase in the second component of facilitation (Figs. 4 and 5), whereas the Ba-induced increase in MEPP frequency is associated mainly with an increase in augmentation (Fig. 6).

Note that the differential effects of Sr^{2+} and Ba^{2+} on transmitter release are clearly evident from a simple inspection of the experimental data; they are not created by the process of analyzing the data in terms of kinetic components. The Sr-induced increase in transmitter release develops during the first 1–2 s of repetitive stimulation (Fig. 5) and decays away in <2 s (Fig. 4 *B*), whereas the Ba-induced increase develops throughout the conditioning stimulation (Fig. 6 *B*) and decays away in ~20 s (Fig. 6 *A*).

Because the faster decaying components are superimposed on the slower ones, it will not be possible to establish whether Sr^{2+} affects the first component of facilitation of MEPP frequency or whether Ba^{2+} affects one or both components of facilitation of MEPP frequency until the relationships between the components of transmitter release are established. In spite of this limitation, the selective effect of Sr^{2+} on the second component of facilitation, with little effect on augmentation and potentiation, and the selective effect of Ba^{2+} on augmentation, with little effect on potentiation, support the suggestion that the components of increased transmitter release are separable and can act relatively independently of one another (see Mallart and Martin [1967], Landau et al. [1973], Magleby [1973], and Magleby and Zengel [1976 *b* and 1976 *c*]). Further support for this suggestion comes from the finding of Erulkar and Rahamimoff (1978) that augmentation of MEPP frequency is abolished in a bathing solution with greatly reduced Ca^{2+}, whereas potentiation of MEPP frequency is not. Erulkar and Rahamimoff (1978) conclude that augmentation and potentiation result from two distinct processes.

Kinetic models that have been developed to describe stimulation-induced changes in EPP amplitude have assumed that changes in transmitter release result from the build up and decay of some factor or factors in the nerve terminal during and after repetitive stimulation (Mallart and Martin, 1967; Linder, 1973; Younkin, 1974). If stimulation-induced changes in spontaneous and evoked transmitter release arise from similar underlying mechanisms, as suggested by the results presented in this paper, then stimulation-induced changes in MEPP frequency provide a measure of the changes in this residual factor (or factors). On this basis, the data in this paper support the major assumption used in the kinetic models. Each nerve impulse does appear to add an increment of residual factor(s), as indicated by the increment in MEPP frequency shown in Fig. 7, which builds up during the train (Figs. 3 *A* and 6 *B*) and then decays with a time-course similar to that of the stimulation-induced changes in EPP amplitude (Figs. 3, 4, and 6; cf. Zengel and Magleby [1980]).

It has been proposed that the residual factor that builds up in the nerve terminal and gives rise to the increase in EPP amplitudes and MEPP frequency is Ca or a Ca complex, Ca^*, and that transmitter release is proportional to the fourth power of Ca^* at the release sites (see Dodge and Rahamimoff [1967], Katz and Miledi [1968], Rahamimoff [1968], Rahamimoff and Yaari [1973], Miledi and Thies [1971]). Since Ca does build up in nerve cells during repetitive stimulation (Baker et al., 1971; Gorman and Thomas, 1978; Ahmed and Connor, 1979; Smith and Zucker, 1980), it is of

some interest to determine whether the fourth-power residual Ca model of transmitter release is consistent with the results obtained in our study.

On the basis of this hypothesis, transmitter release is given by

$$release = k(Ca^*)^4, \tag{3}$$

where k is a constant and Ca^* represents Ca^{2+} or a Ca complex at the release sites. Ca^* may be divided into

$$Ca^* = Ca_S + Ca_E + Ca_R, \tag{4}$$

where Ca_S is the steady-state level of Ca^* in the absence of repetitive stimulation and gives rise to the Ca-dependent resting MEPP frequency, Ca_E represents the transient increase in Ca^* at the release sites at the time of the nerve impulse and gives rise to EPPs, and Ca_R represents the increase in residual Ca^* that builds up during repetitive stimulation and gives rise to the stimulation-induced increase in EPP amplitude and MEPP frequency. By substituting this expression for Ca^* into Eq. 3, transmitter release is given by

$$release = k(Ca_S + Ca_E + Ca_R)^4, \tag{5}$$

where transmitter release is expressed in quanta/s and includes both phasic release, which produces EPPs, and tonic release, which produces MEPPs.

As pointed out by Miledi and Thies (1971), it is possible to use a single equation of this type to include both EPP amplitude and MEPP frequency if EPP amplitude is expressed in quanta/s rather than quantal content. For example, if it is assumed that the phasic transmitter release that follows the transient increase in Ca_E at the time of the nerve impulse lasts about 1 ms (Katz and Miledi, 1965), then the phasic release rate during this 1-ms period would be 1,000 quanta/s if the nerve impulse released a single quantum of transmitter.

Under the conditions of our experiments, a single nerve impulse in the absence of repetitive stimulation ($Ca_R = 0$) did typically release about 1 quantum of transmitter. The value of Ca_E is not known under these conditions, but if Ca^* is expressed in units and Ca_E is set equal to 1 unit for 1 ms at the time of each impulse (phasic release) and set equal to 0 at all other times (tonic release), then the value of k in Eq. 5 would be 1,000 quanta/s if Ca_S is small when compared with Ca_E, a likely condition.

To account for the four components of increased MEPP frequency and EPP amplitude with the fourth-power residual Ca model described by Eq. 5, it is necessary to assume that Ca_R is sequestered or removed in such a manner as to give four apparent components with different time constants and that Ba^{2+} and Sr^{2+} can selectively affect some components without affecting others. (A discussion of restrictions that would apply to assumptions of this type is presented in Zengel and Magleby [1980].) To simplify the initial evaluation of Eq. 5, we will assume that there is only one component of increased transmitter release.

Fig. 8 *A* and *B* shows the decay of EPP amplitude and MEPP frequency calculated with Eq. 5, assuming that Ca_R built up to 20% of Ca_E during a

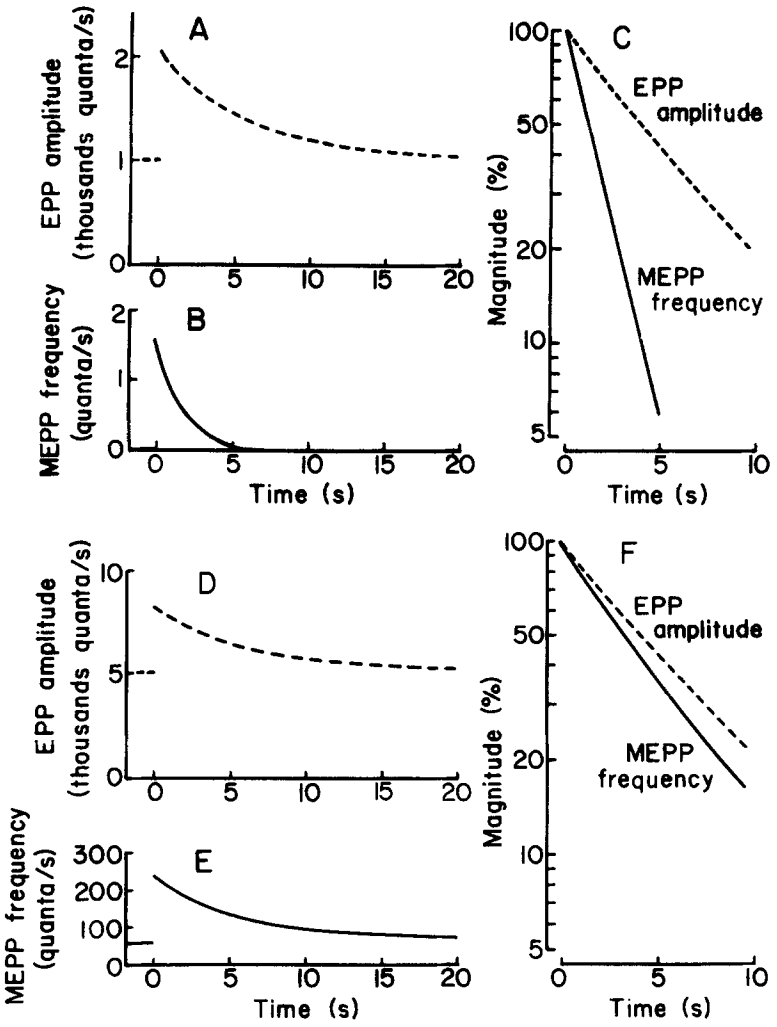

FIGURE 8. Relationship between the decay of MEPP frequency and EPP amplitude predicted on the basis of the fourth-power residual calcium hypothesis of transmitter release described by Eq. 5. (*A* and *B*) Calculated decay of evoked transmitter release (EPP amplitude) and MEPP frequency, assuming that Ca_R increases from 0 to 0.2 at 0 time and then decays away with a 7-s time constant; Ca_E = 1 and Ca_S = 0.001. (*C*) Semilogarithmic plots of the decays of the fractional increase in EPP amplitude and MEPP frequency obtained from *A* and *B*. (*D–F*) Same as *A–C* except Ca_S = 0.5.

train (Ca_R = 0.2) and then decayed with a 7-s time constant and that Ca_S was small when compared with Ca_E (Ca_S = 0.001). Fig. 8 *C* presents semilogarithmic plots of the decays of the fractional increase in EPP amplitude and MEPP frequency. Notice that the fourth-power residual Ca model predicts that MEPP frequency should decay ~3.4 times faster than EPP amplitude

under these conditions. This theoretical finding is in marked contrast to the experimental observation that analogous components of increased MEPP frequency and EPP amplitude decayed at about the same rate (Table I).

If we assumed that Ca_S was not so small when compared with Ca_E but equaled 1 or 10% of Ca_E (Ca_S = 0.01 or 0.1, respectively), then the calculated decay rates of MEPP frequency were still 3.1 or 2.2 times faster, respectively, than the calculated decay rates of EPP amplitudes (not shown). If Ca_S were set equal to 50% of Ca_E (Ca_S = 0.5), the calculated decay rates of MEPP frequency and EPP amplitudes were somewhat similar, although MEPP frequency still decayed slightly faster, as shown in Fig. 8 *D–F*. Under these conditions, however, the predicted MEPP frequency in the absence of repetitive stimulation was 62.5/s, more than 100 times greater than the resting MEPP frequency of ~0.5/s observed in our experiments. It seems unlikely that any error in estimating the value of k from the resting quantal content would be large enough to account for this 100-fold discrepancy, and, if the value of k were arbitrarily changed to describe the resting MEPP frequency, Eq. 5 would no longer describe resting quantal content. Thus, the fourth-power residual Ca model described by Eq. 5 cannot account for the decay of MEPP frequency and EPP amplitude, the resting quantal content, and resting MEPP frequency all at the same time.

The fourth-power residual Ca model can be further tested by determining whether it can account for the relationship between EPP amplitude and MEPP frequency during repetitive stimulation when both types of transmitter release are increasing. Fig. 9 *A* presents plots of the observed increase in EPP amplitude against time during conditioning stimulation of 200 impulses at 20/s (experiment also illustrated in Fig. 3). The continuous line in Fig. 9 *B* is a plot of the predicted increase in MEPP frequency during the train calculated with Eq. 5, assuming k = 1,000 quanta/s, Ca_S = 0.001, and using values of Ca_R calculated from the observed increase in EPP amplitude. For this calculation we assumed that the resting (spontaneous) MEPP frequency in the absence of repetitive stimulation was essentially Ca independent by letting Ca_S be small. The dashed line in Fig. 9 *B* is a plot of predicted MEPP frequency, assuming k = 100 quanta/s and Ca_S = 0.17. For this calculation, resting MEPP frequency was assumed to be Ca dependent by selecting values of k and Ca_S that gave the observed resting MEPP frequency of 0.8/s. For both of these cases, the fourth-power residual Ca model predicted that average MEPP frequency would increase with a pronounced upward inflection during the conditioning train, reaching a rate of 150/s after 10 s of stimulation. The predicted response is inconsistent with the observed increase in MEPP frequency during the conditioning stimulation, which did not inflect upward and which reached an average frequency of 10/s (Fig. 9 *C*). Changing the values of Ca_S and k used in the calculations could change the form of the predicted response or scale it, respectively, but it was not possible to select plausible values for these parameters that would simultaneously give the observed form of the response and the observed MEPP frequencies.

The data in Fig. 9 *A* and *C* represent the average response of 12 cells. When

the data from single endplates were analyzed separately, the form of the response varied at the different endplates but similar results were obtained in all cases; predicted MEPP frequency increased markedly slower than the observed MEPP frequency during the first few seconds of stimulation and then increased much more rapidly than the observed MEPP frequency after this time.

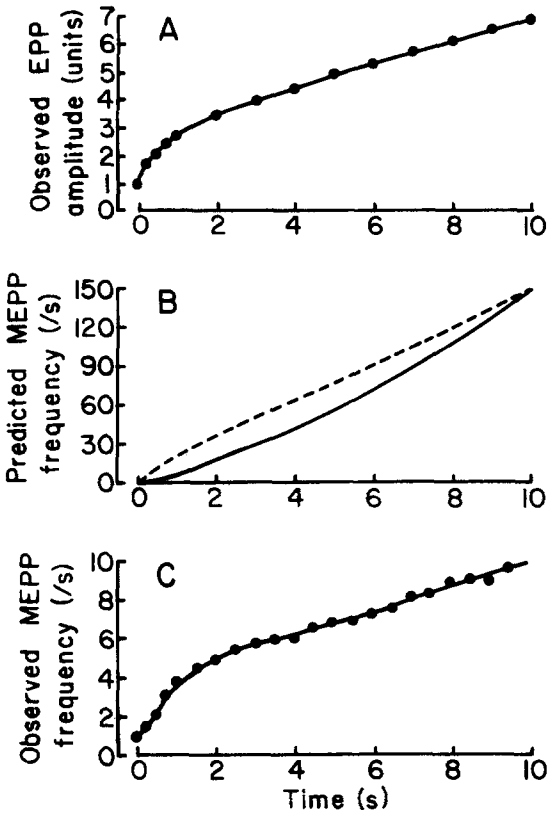

FIGURE 9. Relationship between MEPP frequency and EPP amplitude during conditioning stimulation. (*A*) Increase in EPP amplitudes during the conditioning train for the experiment presented in Fig. 3. (*B*) Predicted increase in MEPP frequency during the train in *A* calculated with Eq. 5 using values of Ca_R determined from the increase in EPP amplitude. Continuous line: k = 1,000 quanta/s, Ca_E = 1, and Ca_S = 0.001. Dashed line: k = 100 quanta/s, Ca_E = 1, and Ca_S = 0.3. (*C*) Observed increase in MEPP frequency during the conditioning train.

Thus, in our experiments the fourth-power residual Ca model described by Eq. 5 cannot account for the relationship between EPP amplitude and MEPP frequency during or after stimulation. It seems unlikely that the lack of fit was due to saturation or depletion phenomena, because the quantal contents

(typically 0.1–1.5) and MEPP frequencies were low. In addition, the concentrations of Ca^{2+} (typically 0.4 mM) and Mg^{2+} (5 mM) used in our experiments would assure that the data were collected within the fourth-power range of the curve relating $[Ca^{2+}]_0$ to transmitter release (Dodge and Rahamimoff, 1967). Note also that Eq. 5 does not specify the source of the residual Ca^* (Ca_R). It could arise by Ca^{2+} entering the nerve terminal and accumulating during repetitive stimulation or by Ca^{2+} release from intracellular stores. In either case, Eq. 5 would be expected to describe the relationship between MEPP frequency and EPP amplitude if the relationships described by it are correct and if the assumption used in evaluating this equation, that Ca_E does not change during repetitive stimulation, is also correct. Although we cannot exclude the possibility that Ca_E may change during the stimulation used in our experiments, available data suggest that Ca_E remains relatively constant (Smith and Zucker, 1980).

One aspect of our data that a power model acts in the right direction to account for is that the increases in MEPP frequency observed in the presence of Ba^{2+} and Sr^{2+} were typically many times greater than the increases in EPP amplitude. For example, during short conditioning trains the increase in MEPP frequency was 20 times greater in the presence of Sr^{2+} than in its absence (Fig. 4 *B*), whereas in a somewhat similar experiment Sr^{2+} increased EPP amplitude only two times (Fig. 7 *B* of Zengel and Magleby [1980]). Calculations with Eq. 5 showed that small increases in Ca_R (Sr_R?) could produce large changes in MEPP frequency while having a lesser effect on EPP amplitude. However, for the reasons pointed out above (Figs. 8 and 9), a fourth-power residual Ca (Sr, Ba) model cannot account for the observations that analogous components of increased MEPP frequency and EPP amplitude decayed at similar rates in the presence and absence of Ba^{2+} and Sr^{2+}, nor can it account for the relationship between EPP amplitude and MEPP frequency during the conditioning trains in the presence of these ions.

The observation that the components of increased transmitter release are separable and can act somewhat independently of one another (Landau et al., 1973; Magleby, 1973; Magleby and Zengel, 1976 *b* and 1976 *c*; Erulkar and Rahamimoff, 1978; Zengel and Magleby, 1980; this paper) is also difficult to explain with the fourth-power residual Ca hypothesis, as is the observation that potentiation appears to accumulate linearly rather than to the fourth power (Magleby and Zengel, 1975 *a* and 1975 *b*).

It appears, then, that to account for all aspects of stimulation-induced changes in transmitter release it will be necessary to modify the fourth-power residual Ca hypothesis described by Eq. 5. It is known that there are a number of different Ca^{2+} buffering and sequestering systems in nerve (Baker and Glitsch, 1975; Blaustein et al., 1978), which may require that the concept of residual Ca be changed from that described by Eqs. 3–5. Furthermore, some components of increased transmitter release may not arise from residual Ca in the classical sense. Erulkar and Rahamimoff (1978) have suggested that augmentation of MEPP frequency is associated with an increased permeability of the nerve terminal membrane to Ca^{2+}.

It may be found that some aspects of increased transmitter release are consistent with the fourth-power residual Ca hypothesis, while others are not. In our experiments, MEPP frequency typically increased with a slight upward inflection during the first few hundred milliseconds of stimulation (Figs. 4 *B*, 5, and 9 *C*), as would be expected if the early onset components of stimulation-induced changes in transmitter release are consistent with this hypothesis. Barrett and Stevens (1972) have found that a fourth-power residual Ca model could account for the relationship between MEPP frequency and EPP amplitude after a single impulse. Considering the conditions of their experiments, which were markedly different from ours in terms of temperature (1–2°C), numbers of conditioning impulses, and conditioning-testing intervals, they were looking mainly at an early component of facilitation. The mechanism of this component may be consistent with Eq. 5, whereas that of the slower components is not, perhaps because the repetitive stimulation required to see these later components leads to accumulation of Na^+ and Mg^{2+} in the nerve terminal, which would be expected to affect transmitter release (Birks and Cohen, 1968; Hurlbut et al., 1971; Atwood et al., 1975; Erulkar and Rahamimoff, 1978). Repetitive stimulation, perhaps through the cumulative action of Ca, could also lead to changes in other factors in the nerve terminal, such as the number of effective release sites and the location of synaptic vesicles. Changes in all of these factors, then, as well as changes in residual Ca and perhaps Ca permeability, could contribute to stimulation-induced changes in transmitter release.

We thank Dr. E. Barrett for helpful discussions.
This research was supported by National Institutes of Health grant NS 10277.
Please address reprint requests to Dr. Karl L. Magleby, Department of Physiology and Biophysics, R 430, University of Miami School of Medicine, Miami, Fla. 33101.

Received for publication 10 September 1980.

REFERENCES

AHMED, A., and J. A. CONNOR. 1979. Measurement of calcium influx under voltage clamp in molluscan neurons using the metallochromaic dye arsenazo III. *J. Physiol (Lond.)*. **286:**61–82.

ATWOOD, H. L., L. E. SWENARCHUK, and C. R. GREUNWALD. 1975. Long-term synaptic facilitation during sodium accumulation in nerve terminals. *Brain Res.* **100:**198–204.

BAKER, P. F., and H. G. GLITSCH. 1975. Voltage-dependent changes in the permeability of nerve membranes to calcium and other divalent cations. *Philos. Trans. R. Soc Lond. B Biol. Sci.* **270:**389–409.

BAKER, P. F., A. L. HODGKIN, and E. B. RIDGWAY. 1971. Depolarization and calcium entry in squid giant axons. *J. Physiol. (Lond.)*. **218:**709–755.

BARRETT, E. F., J. N. BARRETT, D. BOTZ, D. B. CHANG, and D. MAHAFFEY. 1978. Temperature-sensitive aspects of evoked and spontaneous transmitter release at the frog neuromuscular junction. *J. Physiol. (Lond.)*. **279:**253–273.

BARRETT, E. F., and C. F. STEVENS. 1972. The kinetics of transmitter release at the frog neuromuscular junction. *J. Physiol. (Lond.)*. **227:**691–708.

BIRKS, R. I., and M. W. COHEN. 1968. The action of sodium pump inhibitors on neuromuscular transmission. *Proc. R. Soc. Lond. B Biol. Sci.* **170:**381–399.

BLAUSTEIN, M. P., R. W. RATZLAFF, N. C. KENDRICK, and E. S. SCHWEITZER. 1978. Calcium buffering in presynaptic nerve terminals. I. Evidence for involvement of a nonmitochondrial ATP-dependent sequestration mechanism. *J. Gen. Physiol.* **72:**15–41.

BOYD, I. A., and A. R. MARTIN. 1956. The end-plate potential in mammalian muscle. *J. Physiol. (Lond.).* **132:**74–91.

BRAUN, M., and R. F. SCHMIDT. 1966. Potential changes recorded from the frog motor nerve terminal during its activation. *Pfluegers Archiv. gesamte Physiol. MenschenTiere.* **287:**56–80.

BRAUN, M., R. F. SCHMIDT, and M. ZIMMERMANN. 1966. Facilitation at the frog neuromuscular junction during and after repetitive stimulation. *Pfluegers Archiv. gesamte Physiol. Menschen Tiere.* **287:**41–55.

CHARLTON, M. P., and G. D. BITTNER. 1978. Presynaptic potentials and facilitation of transmitter release in the squid giant synapse. *J. Gen. Physiol.* **72:**487–511.

DEL CASTILLO, J., and B. KATZ. 1954 *a*. Quantal components of the end-plate potential. *J. Physiol. (Lond.).* **124:**560–573.

DEL CASTILLO, J., and B. KATZ. 1954 *b*. Statistical factors involved in neuromuscular facilitation and depression. *J. Physiol. (Lond.).* **124:**574–585.

DENNIS, M. J., and R. MILEDI. 1974. Characteristics of transmitter release at regenerating frog neuromuscular junctions. *J. Physiol. (Lond.).* **239:**571–594.

DODGE, F. A., and R. RAHAMIMOFF. 1967. Cooperative action of calcium ions in transmitter release at the neuromuscular junction. *J. Physiol. (Lond.).* **193:**419–432.

ERULKAR, S. D., and R. RAHAMIMOFF. 1978. The role of calcium ions in tetanic and post-tetanic increase of miniature end-plate potential frequency. *J. Physiol. (Lond.).* **287:**501–511.

FENG, T. P. 1941. Studies on the neuromuscular junction. XXVI. The changes in the end-plate potential during and after prolonged stimulation. *Chin. J. Physiol.* **16:**341–372.

GAGE, P. W., and J. I. HUBBARD. 1966. An investigation of the post-tetanic potentiation of end-plate potentials at a mammalian neuromuscular junction. *J. Physiol. (Lond.).* **184:**353–375.

GORMAN, A. L. F., and M. V. THOMAS. 1978. Changes in the intracellular concentration of free calcium ions in a pace-maker neuron, measured with the metallochromic indicator dye arsenazo III. *J. Physiol. (Lond.).* **275:**357–376.

HUBBARD, J. I. 1963. Repetitive stimulation at the mammalian neuromuscular junction, and the mobilization of transmitter. *J. Physiol. (Lond.).* **169:**641–662.

HURLBUT, W. P., H. B. LONGENECKER, JR., and A. MAURO. 1971. Effects of calcium and magnesium on the frequency of miniature end-plate potentials during prolonged tetanization. *J. Physiol. (Lond.).* **219:**17–38.

KATZ, B., and R. MILEDI. 1965. The effect of temperature on the synaptic delay at the neuromuscular junction. *J. Physiol. (Lond.).* **181:**656–670.

KATZ, B., and R. MILEDI. 1968. The role of calcium in neuromuscular facilitation. *J. Physiol. (Lond.)* **195:**481–492.

KATZ, B., and S. THESLEFF. 1957. On the factors which determine the amplitude of the 'miniature end-plate potential.' *J. Physiol. (Lond.).* **137:**267–278.

KRIEBEL, M. E., and C. E. GROSS. 1974. Multimodal distribution of frog miniature endplate potentials in adult, denervated, and tadpole leg muscle. *J. Gen. Physiol.* **64:**85–103.

LANDAU, E. M., A. SMOLINSKY, and Y. LASS. 1973. Post-tetanic potentiation and facilitation do not share a common calcium-dependent mechanism. *Nat. New Biol.* **244:**155–157.

LARGE, W. A., and H. P. RANG. 1978. Factors affecting the rate of incorporation of a false transmitter into mammalian motor nerve terminals. *J. Physiol. (Lond.).* **285:**1–24.

LILEY, A. W. 1956. The quantal components of the mammalian end-plate potential. *J. Physiol. (Lond.).* **133:**571–587.

LINDER, T. M. 1973. Calcium and facilitation at two classes of crustacean neuromuscular synapses. *J. Gen. Physiol.* **61**:56–73.

MAGLEBY, K. L. 1973. The effect of tetanic and post-tetanic potentiation on facilitation of transmitter release at the frog neuromuscular junction. *J. Physiol. (Lond.)*. **234**:353–371.

MAGLEBY, K. L., and J. E. ZENGEL. 1975 *a*. A dual effect of repetitive stimulation on post-tetanic potentiation of transmitter release at the frog neuromuscular junction. *J. Physiol. (Lond.)*. **245**:163–182.

MAGLEBY, K. L., and J. E. ZENGEL. 1975 *b*. A quantitative description of tetanic and post-tetanic potentiation of transmitter release at the frog neuromuscular junction. *J. Physiol. (Lond.)*. **245**:183–208.

MAGLEBY, K. L., and J. E. ZENGEL. 1976 *a*. Augmentation: a process that acts to increase transmitter release at the frog neuromuscular junction. *J. Physiol. (Lond.)*. **257**:449–470.

MAGLEBY, K. L., and J. E. ZENGEL. 1976 *b*. Long-term changes in augmentation, potentiation, and depression of transmitter release as a function of repeated synaptic activity at the frog neuromuscular junction. *J. Physiol. (Lond.)*. **257**:471–494.

MAGLEBY, K. L., and J. E. ZENGEL. 1976 *c*. Stimulation-induced factors which affect augmentation and potentiation of transmitter release at the frog neuromuscular junction. *J. Physiol. (Lond.)*. **260**:687–717.

MALLART, A., and A. R. MARTIN. 1967. An analysis of facilitation of transmitter release at the neuromuscular junction of the frog. *J. Physiol. (Lond.)*. **193**:679–694.

MARTIN, A. R., and G. PILAR. 1964. Presynaptic and post-synaptic events during post-tetanic potentiation and facilitation in the avian ciliary ganglion. *J. Physiol. (Lond.)*. **175**:17–30.

MCLACHLAN, E. M. 1977. The effects of strontium and barium at synapses in sympathetic ganglia. *J. Physiol. (Lond.)*. **267**:497–518.

MELLOW, A. M., T. E. PHILLIPS, and E. M. SILINSKY. 1978. On the conductance pathways traversed by strontium in mediating the asynchronous release of acetylcholine by motor nerve impulses. *Br. J. Pharmacol.* **63**:229–232.

MILEDI, R., and R. THIES. 1971. Tetanic and post-tetanic rise in frequency of miniature end-plate potentials in low-calcium solutions. *J. Physiol. (Lond.)*. **212**:245–257.

RAHAMIMOFF, R. 1968. A dual effect of calcium on neuromuscular facilitation. *J. Physiol. (Lond.)*.**195**:471–480.

RAHAMIMOFF, R., and Y. YAARI. 1973. Delayed release of transmitter at the frog neuromuscular junction. *J. Physiol. (Lond.)*. **228**:241–257.

SILINSKY, E. M. 1978. On the role of barium in supporting the asynchronous release of acetylcholine quanta by motor nerve impulses. *J. Physiol. (Lond.)*. **274**:157–171.

SILINSKY, E. M., A. M. MELLOW, and T. E. PHILLIPS. 1977. Conventional calcium channel mediates asynchronous acetylcholine release by motor nerve impulses. *Nature (Lond.)*. **270**: 528–530.

SMITH, S. J., and R. S. ZUCKER. 1980. Aequorin response facilitation and intracellular calcium accumulation in molluscan neurons. *J. Physiol. (Lond.)*. **300**:167–196.

YOUNKIN, S. G. 1974. An analysis of the role of calcium in facilitation at the frog neuromuscular junction. *J. Physiol. (Lond.)*. **237**:1–14.

ZENGEL, J. E., and K. L. MAGLEBY. 1977. Transmitter release during repetitive stimulation: selective changes produced by Sr^{2+} and Ba^{2+}. *Science (Wash. D. C.)*. **197**:67–69.

ZENGEL, J. E., and K. L. MAGLEBY. 1978. Spontaneous and evoked transmitter release share some common mechanisms. *Biophys. J.* **21**:51 *a*. (Abstr.).

ZENGEL, J. E., and K. L. MAGLEBY. 1980. Differential effects of Ba^{2+}, Sr^{2+}, and Ca^{2+} on

stimulation-induced changes in transmitter release at the frog neuromuscular junction. *J. Gen. Physiol.* **76:**175–211.

ZUCKER, R. S. 1974. Crayfish neuromuscular facilitation activated by constant presynaptic action potentials and depolarizing pulses. *J. Physiol. (Lond.).* **241:**69–89.

ZUCKER, R. S., and L. O. LARA-ESTRELLA. 1979. Is synaptic facilitation caused by presynaptic spike broadening? *Nature (Lond.).* **278:**57–59.